

RLaMs Optimized Depth Map Improvement Single Colour Image Dehazing

Abstract-Visibility Degradation is a classical problem owing to the presence of Atmospheric Particulate Matter (APM). There are different image dehazing algorithms. Any one method cannot be relied upon as each haze condition is unique in nature. An innovative algorithm has been proposed with the help of image formation atmospheric scattering model. The model has been improvised by one key factor. This is Regularized Lagrangian multiplier (RLaM) based Depth Map (DM) refinement. The algorithm has low time complexity which intrigue in real time efficient applications. Different state-of-the art visibility algorithms have been studied and their subjective and objective performance evaluations have been evaluated. Extensive investigation shows remarkable improvement with the proposed algorithm. This method is equally applicable for different atmospheric conditions. Time has been evaluated both by execution time as well as by time complexity Big (O) notation. The resultant images are visibly clear satisfying the criteria for computer vision applications. It is evident from the experimental results that the proposed technique is effective and applicable for real time. Lastly ringing artifacts are removed efficiently.

Keywords- Airlight, Transmission estimation, APM, Ill-Posed Inverse Problem, Big (O)

1. Introduction

APM is a real threat in our green world. Researchers are fighting against it. One of the reasons of APM is unplanned civilization and technological advancements. It has been observed from satellite images that Asian and African and very few parts of American countries are the most polluted places. Image sources from satellites show year wise degradation .APM are both natural and manmade. APM are a mixture of solid and liquid droplets. They are in variety of sizes. Coarse APM ranges PM_{10} - $PM_{2.5}$ (micrometre diameter), finer are below $PM_{2.5}$ and ultrafine below $PM_{0.1}$ [1]. Computer vision (CV) is a promising branch of technology which encompasses object tracking, object recognition, surveillance, image enhancement etc. Clear image is an essential requirement in CV. But APM degrades visibility of the received image. Rain, fog, vog, mist, fume, smog, hail, snow etc. are the cause of visibility reduction in image. Outdoor image is a challenge in computer vision, especially in bad weather condition. Image formation at the viewer point (i.e. may be considered camera) is influenced by distance, airlight, transmission, and scattering coefficient [2]. There are some classical enhancement techniques, like, histogram equalization, imadjust, adaptive histogram equalization. These techniques work well in most of the cases. In some special cases (like, fog, haze, smoke, rain, vog etc.) these techniques fail. In those special cases of bad weather nothing can be seen from the image. The situation becomes worsen if no ground truth or reference image could be found. In these contexts special popular algorithms have to be selected. Those are working with no ground truth image or popularly called single image dehazing algorithms. The key observations found from outdoor haze free images are as i) image contrast of normal image is high, ii) airlight does not affect the richness of the image, iii) pixels intensity is well distributed in the intensity scale, and iv) pixel over-saturation and under saturation do not exist[22]. Contrary to that of hazy images are of low contrast and airlight makes images white. Most of the pixel intensities are very high i.e., under-saturated and flocked together. Degraded image pixels are over saturated in one of the channels. The cause may be due to the illuminant of strong colour cast or sensor/camera respond differently for different colour channels. Resultant of these artifacts makes image pixels achromatic. Visibility Improvement is under the category of Ill-Posed Inverse Problem. In this class best or optimum image has to be extracted from a series of attenuated received images. Sometimes it is extremely difficult to retrieve any information about the original image as the problem becomes Ill-Posed Inverse Problem [3]. Paper is arranged as below. Section II consists of Literature survey. Main contribution of the work has been identified in section 3. Proposed methods with mathematical modelling have been illustrated Section 4. Result is described in section V. Section VI explains qualitative and quantitative analysis. Section VII elaborates its applications and type of device used for the research. Finally section VIII is for Conclusion.

2. Background and Associated Work

In some research work DCP (dark channel prior) has been used which is a statistical prior on haze free images. This prior indicates that in normal RGB image 75% pixels of any dark channel is zero where dark channel indicates the lowest intensities channel out of three RGB image channel. 90% pixels of that channel are below 25. However the scenario drifts radically in case of degraded weather. That corresponds to high intensity of dark channel. It is due to atmospheric airlight which shifts the pixels intensity to very high value producing almost white image. The method is efficient, but takes long time to reproduce. Therefore for real time application cannot be useful [4]. The work of R Tan based on two observations, contrast of image is compromised in degraded image. Normal image has more contrast than that of hazy image. Degraded image has more airlight and it increases with distance. As a result distant part becomes smoother and invisible. The method is efficient as required single image, but not applicable for real time [5]. The algorithm proposed by J P Tarel is fast and its complexity is linear function with the number of image pixels for both colour and gray image. The algorithm is tuned by only four parameters, atmospheric veil inference, image restoration, smoothing, and tone mapping [6]. Research work of R Fattal based on haze estimation, scatter light estimation. From that information haze free image contrast has been recovered. It has been assumed that transmission and surface shading is locally uncorrelated. This simple statistical assumption reduces other complexity like surface albedo. The challenge of this method is to solve the pixels where no transmission is available. Implicit graphical model made it possible to extrapolate solution of those pixels[7]. It is not a patch based prior contrary to previous methods. It is non-local prior. D Berman et. al. emphasised that degradation is not uniform. It is different for different pixels of the image and is controlled by transmission coefficient. It has been proposed colours of haze free to be clustered and spread over the entire image. Whereas hazy image forms line of colours that was earlier clustered, called haze line. It recovers distance map. The algorithm is linear, faster, deterministic, no training required [8]. Authors are working on visibility improvements. Their earlier works were DCP based vision improvement where speed of the original algorithm was improved with reduced complexity and sky masking [9]. In [10] authors proposed three algorithms and revised DCP by gamma correction, contrast controller, sky masking and guided filtering. In [11, 12, and 13] authors emphasised on objective evaluation of DCP method and mathematical modeling of image formation. DCP is basically patch based or local prior. Patch size in [4] was 15x15, omega was 0.95. These two parameters play a significant role. This has been shown [14]. DCP with sky masking is a useful algorithm. But the value of optimum value is difficult to find out. It is evaluated manually. In [5] this difficulty has been recovered by using Cuckoo Search Algorithm. Resultant image using CSA removes the artifacts of sky reflection very well. Visibility Improvement is a classical Inverse problem. Haze is always associated with blurring. Here both have been treated and removed [16,3].

3. Main Contribution of the paper

As discussed above single image colour dehazing is a challenge and complex in nature. In this work low complexity depth map non-linear noise removal model has been estimated. Image degradation optical model with refined transmission via RLaMs depth map estimation produces the resulting reconstructed output. Apart from that haziness factor k has been evaluated automatically depending on the spread of intensity in the depth map [WLMS based automated haze removal].

3.1 Regularized Lagrange Multiplier (RLaM) and Point Spread Function(PSF)

Blur is an integral part of any degraded image. It comes along with nonlinear noise. The degrading system prior model has to be reconstructed from blur or degraded image. Linear filters like Wiener, Least square filter, and nonlinear filter like Lucy Richardson filter have also been studied. RLaMs have been applied to remove blur which has been compared to classical methods using parametric assessment of PSNR and time consumed [24, 25]. RLaMs are effective and important in computer graphics applications as it is non-iterative, fast, and bypass the problem of parameterizing system's degree of freedom. Finally it has computational complexity $O(n)$. [28]. These advantages of LaMs have been adapted in this research work.

The PSF is a quantity to determine the power of an optical system. Better resolution may be achieved by narrowing the PSF. It is the spread of a point source of light as it passes through a system. Ideally a point source in space is defined by delta function infinite spectrum in special frequency k_x, k_y . PSF of an image forming optical system is resolved by the parameter of optical system and the distance or depth of the object to be imaged [29]. Figure 3 shows PSF(Point Spread Function) with Gaussian kernel 3x3 and standard deviation 10, noise variance 0.1. Twelve different outdoor natural degraded images have been recovered with Regularized Lagrange Multiplier with the above PSF. It is often encountered in engineering and science applications the discretization of linear ill-conditioned problems. This leads to large ill-conditioned linear systems with right hand side corrupted by noise [27]. The solution of this kind of linear system needs the solution of a minimizing problem which is dependent on the estimation of the variance of the noise. This approach is well-known as regularization. Lagrangian is a technique to solve this type of Noise Constrained Regularization problem.

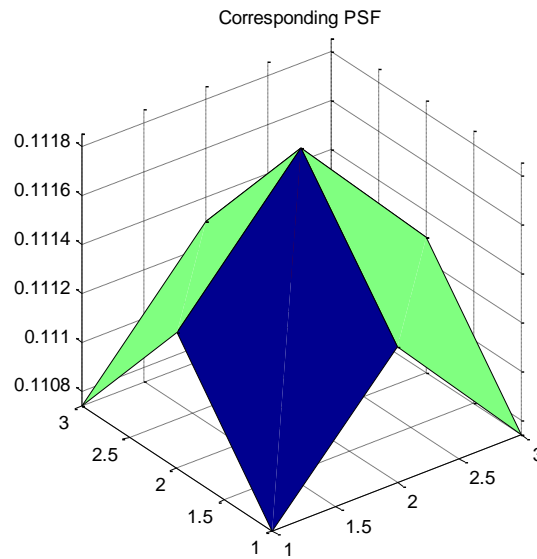


Fig. 1 Point Spread Function used with Gaussian kernel 3x3 and standard deviation 10, noise variance 0.1.

3.2 Image Formation Process

Initially image restoration method is considered under the category of linear spatially invariant restored filters. Blurring function is considered as point spread function (PSF) or convolution kernel $h(n_1, n_2)$. Statistical properties (mean, correlation) of the original image are assumed to be non-changeable spatially. Under these conditions image formation mathematical model is formulated. Here $f(n_1, n_2)$ is the ideal spatially discrete image with no blur or noise. The received image is displayed as

$$\begin{aligned}
 g(n_1, n_2) &= h(n_1, n_2) * f(n_1, n_2) & 3.2.1 \\
 &= \sum_{k_1=0}^{N-1} \sum_{k_2=0}^{M-1} h(k_1, k_2) f(n_1 - k_1, n_2 - k_2)
 \end{aligned}$$

The above equation can be rewritten in matrix form. $F \in \mathbb{R}^{r \times n}$ is the matrix form of original image. $G \in \mathbb{R}^{r \times m}$ is the corresponding degraded image. $f_{i,j}$ is the pixel elements $i=1, \dots, r$ and $j=1, \dots, n$. $H \in \mathbb{R}^{m \times n}$ is the degradation matrix. Each row of matrix are related by

$$g = Hf, \quad g \in \mathbb{R}^m, \quad f \in \mathbb{R}^n, \quad H \in \mathbb{R}^{m \times n} \quad 3.2.2$$

Where $f = f_i^T$ and f_i represents i th row of the original image F . Similarly $g = g_i^T$ and g_i represents i th row of the degraded image G . The process is repeated for each row of the matrix and develops an unknown system of m simultaneous equations with $n=m+l-1$. It is now easy to evaluate PSF which is assumed to be spatially invariant, and the degradation matrix H with zero boundary conditions. It is assumed that the length of blur be l in pixels which is also known as degradation index and an integer. Degradation index ' l ' is very difficult to find and has to be approximated from the degraded image. Degradation index ' l ' can be recovered by two methods i) one dimensional cepstral method, ii) two dimensional cepstral method. It is now important to find i^{th} row of the blurred image from the i^{th} row of the original image using the eq 4.2.

$$\begin{bmatrix} g_{i,1} \\ g_{i,2} \\ g_{i,3} \\ \vdots \\ \vdots \\ g_{i,m} \end{bmatrix} = \begin{bmatrix} h_1 & \dots & h_l & 0 & 0 & 0 & 0 \\ 0 & h_1 & \dots & h_l & 0 & 0 & 0 \\ 0 & 0 & h_1 & \dots & h_l & 0 & 0 \\ 0 & 0 & 0 & h_1 & \dots & h_l & 0 \\ 0 & 0 & 0 & 0 & h_1 & \dots & h_l \end{bmatrix} \begin{bmatrix} f_{i,1} \\ f_{i,2} \\ f_{i,3} \\ \vdots \\ \vdots \\ f_{i,m} \end{bmatrix} \quad 3.2.3$$

Where $h_i = \frac{1}{l}$ for $i = 1, \dots, l$, h_i is the element of H matrix. The main objective is to retrieve original image from degraded image G and priori knowledge of degraded phenomena matrix H . The matrix $\in \mathbb{C}^{r \times m}$, blurred image, can be written mathematically

$$g_{i,j} = \frac{1}{l} \sum_{k=0}^{l-1} f_{i,j+k}, \quad i = 1 \dots r, j = 1 \dots m \quad 3.3.4$$

Now eq 4.4 can be rewritten as

$$G = (HF^T)^T = FH^T, G \in \mathbb{R}^{r \times m}, H \in \mathbb{R}^{m \times n}, F \in \mathbb{R}^{r \times n} \quad 3.3.5$$

It is clear that there are infinite of exact solutions for f satisfying the eq 4.2 and 4.5. Out of them sharpest restored matrix is essential. The vertical blur matrix is given by

$$G = HF, G \in \mathbb{R}^{m \times n}, H \in \mathbb{R}^{m \times r}, F \in \mathbb{R}^{r \times n}, r = m + l - 1 \quad 3.3.6$$

Now this is assumed that blurring of rows is independent of blurring of columns in image. Consequently there exists two matrices H_c and H_r . In such a scenario these can be expressed as

$$G = H_c F_r^T, G \in \mathbb{R}^{m_1 \times m_2}, H_c \in \mathbb{R}^{m_1 \times r}, F \in \mathbb{R}^{r \times n}, H_r \in \mathbb{R}^{m_2 \times n} \quad 3.3.7$$

Where $n=m_2+l_1-1$, $r=m_1+l_2-1$, l_1 is linear horizontal blur in pixel, and l_2 is linear vertical blur in pixel.

3.3 Image Recovery by Regularized Lagrange Multiplier

In this section an excellent method has been reviewed known as Lagrange Multiplier (LM). This is a linear blur model. The main purpose of the LM is to remove linear blur and recover original image as optimum as possible [fumi]. It is assumed that blur length is integer number of pixels and resolution of the recovered image is very high. From eq 4.2 $g=Hf$, where f is the first ' m ' components of ' f ' which has minimum distance from measured data, $\|\tilde{f} - g\| \rightarrow \min$ 5.1. Now it is assumed that $\tilde{f}=Pf$. P is a $m \times n$ matrix to project f using the backing of g .

$$P = [I_m \mid O] \quad 3.3.1$$

Where I_m denotes identity matrix of size $m \times m$ and O signifies $m \times (l-1)$ null matrix. Eq 5.1, original optimization problem, is redefined as

$$\min_f \|Pf - g\| \quad 3.3.2$$

While subject to constrain $\|Hf - g\|^2 = 0$ 5.4 . Therefore eq 5.3, 5.4 is a constrain optimization problem. Using LMs an alternate optimization problem without constrain can be modelled.

$$V(f) = \lambda \|Hf - g\|^2 + \|Pf - g\|^2 \rightarrow \min \quad 3.3.3$$

λ is known as Lagrange multiplier. Equation 5.5 is strictly convex and low semi continuous with respect to weak-star bounded space topology [24, 25, 26]. Now partial derivative of V with respect to unknown f for very high λ :

$$\frac{\delta}{\delta f} V(f) = 2\lambda H^T (Hf - g) - 2P^T (Pf - g) = 0 \quad 3.3.4$$

$$\check{f} = (\lambda HH^T + P^T P)^{-1} (\lambda H + P)^T g \quad 3.3.5$$

The solution of eq 5.7 in the matrix form is:

$$\check{F} = G(\lambda H + P)((\lambda HH^T + P^T P)^{-1})^T \quad 3.3.6$$

The eq 5.8 interprets the solution of recovered image in the horizontal blurring condition. In case of vertical blurring scenario equation 4.6 and 5.7 will be helpful.

$$\check{F} = (\lambda H^T H + P^T P)^{-1} (\lambda H + P)^T G \quad 3.3.7$$

Now for a two dimensional separable blurring processes the recovered image is:

$$\check{F} = (\lambda H^T H + P^T P)^{-1} (\lambda H + P)^T G (\lambda H + P)((\lambda HH^T + P^T P)^{-1})^T \quad 3.3.8$$

3.4 Time Complexity

There are numerous algorithms to solve a specific problem. Out of several algorithms, one of them has to be chosen. There are also several criteria to fit one algorithm for a problem. **Efficiency** criteria will meet and fit for algorithmic fitness selection in computational computing. Efficiency encompasses three criteria: i) time efficiency, ii) space efficiency, and iii) Development efficiency [30]. In this work we stress on time complexity in terms of execution time and big oh notation. Time complexity in terms of executing time and Big oh notation is one way of classifying and comparing algorithms.

4. Single Colour Image Restoration

Using the above described techniques a novel algorithm has been effectively designed to remove atmospheric turbulence as well as system degradation on single colour image. Total algorithm with their detail mathematical modelling is given below in the corresponding sub-sections.

4.1 Proposed Methodology

In this paper novel algorithm has been framed. The algorithm is based on H Koschmieder and E J McCartney image formation optical model [2,39] and the followed by YCbCr correction . They are elaborated below.

	Input Hazy Image	Computational Complexity
Step I	Average of minimum of three channels as I_{\min}	$O(n)$
Step II	Average of maximum value of three channels as I_{\max}	$O(n)$
Step III	Haziness factor, $k = I_{\min} / I_{\max}$	$O(n)$
Step IV	Airlight Estimation	$O(n)$
Step V	Estimation of minimum intensity channel	$O(n)$
Step VI	Refinement / noise removal of minimum intensity channel by Regularized Lagrange Multiplier Technique (used as Depth Estimation) [28]	$O(n)$
Step VII	Transmission Estimation from step VII	$O(n)$
Step VIII	Recovery of Dehazed image with image degradation optical model [2, 38, 39]	$O(n)$
Step IX	YCbCr correction	$O(n)$
Step X	Evaluation of contrast k , β and d_{\max} of the Dehazed Image	$O(n)$

Fig. 2. Proposed Algorithm

Image formation model, also known as airlight scattering model, was proposed by H Koschmieder, and E J McCartney[2,39] and represented by equation (4.1.1). Basically this model describes how image is degraded at a distance from the original image source. $I(x)$ is the hazy image, $J(x)$ is the haze-free image, $t(x)$ is the transmission map, and it is extremely ill-posed. A denotes atmospheric light. x denotes any pixel of the image. β is atmospheric extinction coefficient and d indicates distance between original image and hazy image or depth of scene. Here I , J , and A are 3-D RGB image array. Only I , the hazy image, is known. A and t have to be estimated to develop good quality dehazed image from hazy image I . Therefore this can be inferred that dehazed image is solely dependent on how close the estimation of A and t to the original one in reality. That is why researchers are effortlessly engaged to develop estimation of A and t as close as the real one.

$$I(x) = J(x)t(x) + A(1 - t(x)) \quad (4.1.1)$$

$$t = e^{-\beta d} \quad (4.1.2)$$

4.2 LMs-based Improved Depth Information estimation

Transmission map is 2-D image array. By minimizing noise present in the transmission image, final dehazed image found is clearer and improved. Transmission map explains the part of light that reaches camera without scattering and minimalizing loss of information pixel-wise. Transmission map is entirely associated with depth

information. If transmission is not estimated properly, halo effect arises. It is a high computational cost problem. Depth map estimation is an earlier step for transmission estimation. Depth map estimation is the understanding of geometric relation in a scene. Depth map estimation from single image is far more harder than multiple images. Instead of using patch-based dark channel[4], minimum of three channels is observed as depth map. This is known as depth map which is severely ill-posed. But it is a raw depth map. It is computationally easy. Images, those are captured by sensors or camera, have to be processed further. Therefore both haze as well as system noise is imposed on the scene radiance. Noise is forced on images during capture and transmission. The resulting output images are under random noise effects. These random noise shifts colour, brightness, sharpness, saturation, and contrast. These errors can be eliminated by RLaMs mentioned earlier in section 3.1.

$$I_{cmin}(x) = \left(\min_{c \in \{r,g,b\}} (I^c(x)) \right) \quad (4.2.1)$$

I^c and I_{cmin} indicate individual channel of RGB image and minimum of three channels I^c respectively. Noise that is found in the minimum intensity channel I_{cmin} can now be used as raw depth map to recover haze free image and easily be made noise free or smoothed by RLaMs technique .

$$I_{cminLMs}(x) = RLMs(I_{cmin}(x)) \quad (4.2.2)$$

Equation (4.2.2) shows noise free minimum intensity channel or refined depth map. This channel is normalised. Compliment of this equation will produce maximum intensity channel with edge preserving smoothing and reduced computational complexity. This is a great advantage. This maximum intensity channel will be applied as the transmission estimation $t(x)$. This transmission is severely ill-posed in nature. By RLaMs this has become well-posed and good quality haze-free image will be generated .Depth map generated by minimum patch estimation which is more accurate, but it is computationally expensive [4]. Whereas this proposed concept is computationally simple and easy to implement.

4.3 Transmission estimation using refined Depth map

Any far point pixel in the minimum intensity channel in the worst case becomes zero. Transmission has been extrapolated from the minimum of three channels shown by equation (4.2.1), instead of patch-based minimum transmission channel which is computationally expensive [4]. Therefore equation (4.1.1) becomes

$$I_{cmin}(x) = A(1 - t(x)) \quad 4.3.1$$

Equation 4.3.1 will be more refined if it may be considered atmospheric light A to be one for the far end point.

The refined equation will be

$$I_{cmin}(x) = 1 - t(x) \quad 4.3.2$$

Another improvement needed as I_{cmin} is noisy and after RLaMs based refinement on depth map estimation according to equation (4.2.2) transmission equation will be rewritten as

$$I_{cminLMS} = LMS(I_{cmin}) \quad 4.3.3$$

$$t_{new}(x) = 1 - I_{cminLMS} \quad (4.3.4)$$

Now after getting refined transmission map for individual image, $t_{new}(x)$ will not be the same for each image, as individual scenario is different. Therefore additional factor, *haziness factor* k, is required to be introduced.

$$t_{new}(x) = 1 - kI_{cminLMS} \quad (4.3.4)$$

k is a proportionality constant for aerial perspective respectively[35,36]. The value of k is between 0 to 1. Zero indicates clear visibility like clear day scene, whereas one indicates absolutely no visibility like thick fog.

4.4 Automated Haziness factor Estimation

$$k = \frac{I_{cmin}}{I_{cmax}} \quad 4.4.1$$

It has already been stated that k, haziness factor, indicates the amount of haze present in the image of interest. So far this is calculated manually by visual inspection of the amount of haze. But for real time application this cannot be implemented. Authors have already working with this [31]. Here it is considered that haziness factor k is the ratio of average of minimum intensity channel to average of maximum intensity channel. This concept works well for real time adaptive visibility improvement.

4.5 Atmospheric Light Estimation

According to the atmospheric scattering model, at the very far distance transmission is almost zero. As a result intensity at that point becomes equal to A, atmospheric light. It is worth to note that distant pixels are maximum bright due to haze. Taking this notion in hand, it has been proposed atmospheric light to be maximum bright pixels. For more robust estimation, atmospheric light A has been considered to be the top 0.1% bright pixels of each channel. An example has been explained in figure 3. It shows degraded image, its depth map and transmission map, recovered image, its depth map, and transmission map by our algorithm. It is evident not only from recovered image, but also from recovered depth map and transmission map that proposed algorithm works well and serves its purpose of cleaning image.

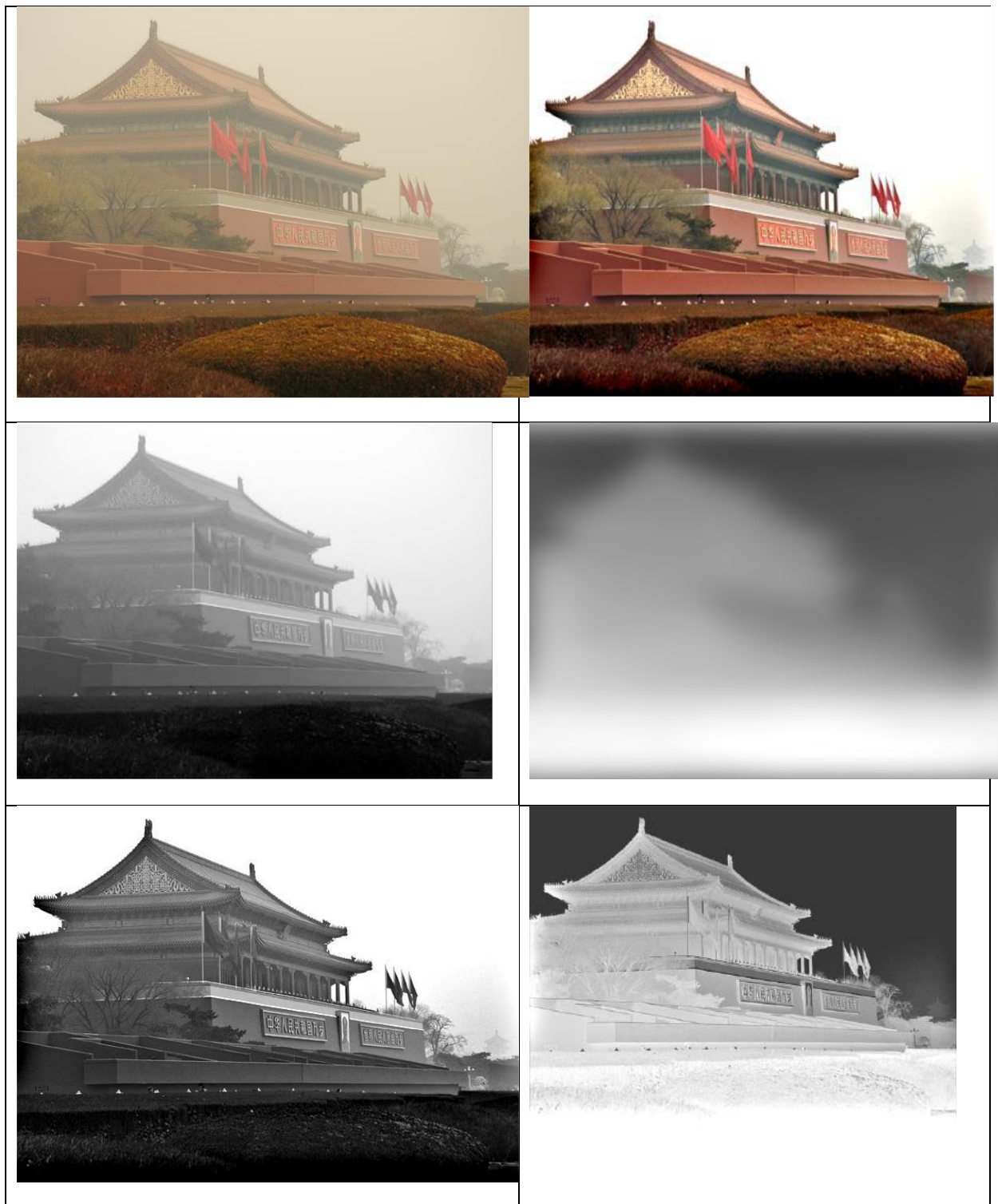


Fig. 3. An overview of the proposed dehazing method. **Top-left:** Dense Input hazy image. **Top-right:** Dehazed image . **Middle -left:** Depth map of hazy image , **Middle –right:** Transmission Map of hazy image, Bottom-Left: Refined Depth map , Bottom- right: Refined Transmission Map

4.6 Scene radiance recovery using scattering image formation optical model

Main objective of the work is to retrieve original hazefree or scene radiance image. Therefore from equation 4.1.1 scene radiance can be recovered. This is shown below.

$$J(x) = \frac{I(x)}{t_{new}(x)} - \frac{A(1 - t(x))}{t_{new}(x)} \quad 4.6.1$$

4.7 YCbCr correction of the scene radiance image

Y is luma or intensity or achromatic colour channel component of any colour image. Cb and Cr are blue difference and red difference respectively. Luminance channel Y is independent of colour information, that is why YCbCr format performs better. By controlling y channel intensity keeping Cb and Cr channels unaffected radiance image brightness may be enhanced, so that gloomy radiance image may be look brighter. This is shown by an example in figure 4. Radiance dehazed image visibility may be enhanced by this YCbCr correction.



Fig. 4. Left: Hazy input, Middle: Scene Radiance, Right: YCbCr correction

5. Experimental Result

In this section the experiment results have been explained with dataset[4] using the proposed algorithm. Two sets of experiments have been conducted. One with single image with different state-of-the-art algorithms and other one is twelve images from [4] data set with the proposed method. For an example, one degraded image has been taken and its depth map and transmission map before and after dehazing have been shown along with recovered image in figure 5. The data set consists of several different images with different depth or haze. For our convenience we resize the images to same size of 70x70 before running the program.

5.1 Qualitative /subjective evaluation

Transmission Map (TM) is an important process in image recovery from haze. Quality of transmission map is essential for good quality output. In this process TMs of He et. al, D Berman, and proposed method have been shown in figure 4.

Method	Depth Map	Transmission
He et. a.		

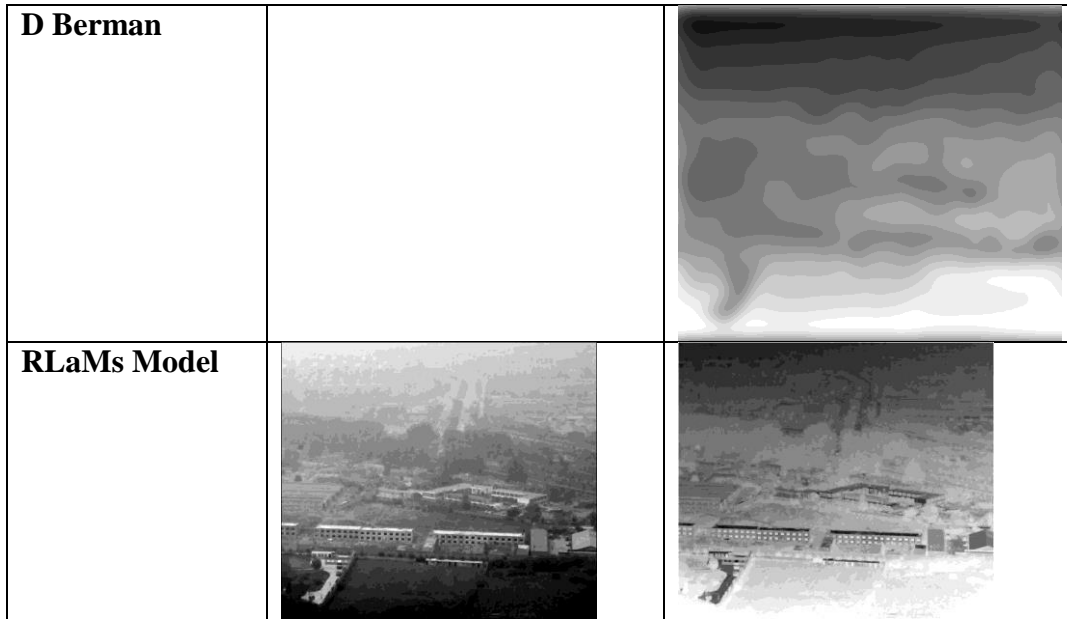


Fig. 5. Transmission map and dark channel of the sample image. Top row : left corner depth map, right corner-transmission map. Middle row: D Berman et. al. left side-depth map, right side-transmission map, Bottom row: RLaMs algorithm, left side-depth map, right side-transmission map.

In figure 5 dark channel and transmission map of sample image have been shown. It is evident that both dark channel and transmission map of the proposed methods are better than that of the work of He *et. al* and D Berman. Individual pixels are operated in our methods. Whereas patch based operation are applied on He *et. al*. method. These patches are prominent in figure 4. This validates that the proposed methods are obviously extracting more information in comparison with other algorithms. Transmission map and dark channel of algorithm by He *et. al*. are unable to extract any original image layout. Whereas transmission map and dark channel of the proposed models produce the original image layout which is the major achievement of the proposed algorithms.

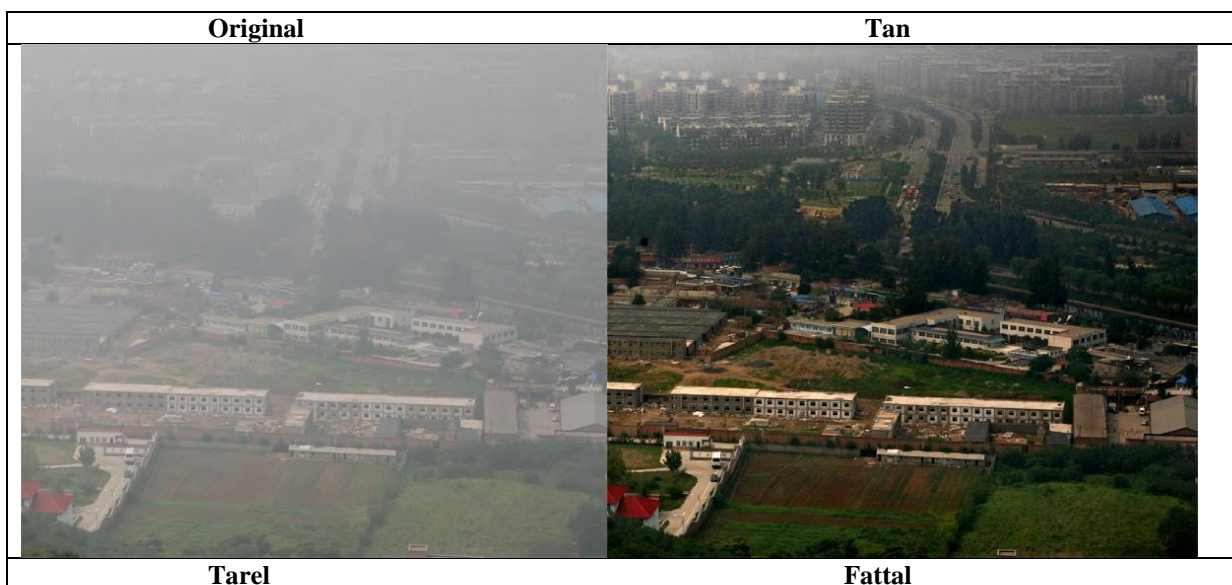




Fig. 6. Comparison of 525x600x3 size Sample Image with different state-of-the art Algorithms

In figure 6 one outdoor long distance image with dense fog has been examined with different recent popular algorithms and their resulting images have been presented. It has been observed that some of them are

performing well and some are not. Visual qualities of the output image of different algorithms are not the same. Result of our proposed algorithms is rich as well as natural looking with low computational complexity. The work[4] is pleasing but dull with high computational complexity.

In figure 7 and figure 8 twelve images from the dataset have been chosen for experiment. Figure 7 is the original images of different degree of haze and figure 8 is the resulting haze-free output from the proposed algorithm.

					
Canon 600x525	City_1 400x600	City_2 600x400	Cones 465x384	Lake 459x321	Ny_1 576x768
					
Ny_2 1024x768	Mountain 600x400	Pumpkins 600x400	Stadium 1000x327	Toys 500x360	Trees 690x464

Fig. 7 Input Poor visibility dataset



Fig. 8. Dehazed images with LMs

It is visibly clear that all the twelve images are artefact free clear images as shown in figure 8 in comparison to figure 7. It is interesting that the said algorithm cleans the images adaptively with different degree of haze. This has been shown in table below.

5.2 Quantitative/ Objective Evaluation:

In [19] N Hautiere *et. Al.* proposed three visibility parameter r , e , and σ referring as the geometric mean of VL, rate of newly visible edge, and normalised newly saturated pixels in the restored image respectively. High values of e and r are appreciated, whereas low value of σ is required. Different existing reputed algorithms along with the proposed work have been evaluated with the above mentioned parameters and other few parameters like PSNR, CNR, CPU execution time, visible edge before and after recovery in table I. It has been found that our method shows satisfactory results in all parametric performance. Here single image as shown in fig 2 is taken as reference. The above table shows few important parameters for image evaluation. These parameters have been applied for evaluation of different well known algorithms performance. It has been found that PSNRs and ' σ ' values of our proposed methods are not the best. Our algorithms show better performance in the parametric evaluation of CNR, VERI, r , e . Finally T (time) consumption of proposed methods outperform all other methods which is the requirement for any other real time application. Therefore this can be said that overall performance of the projected algorithms is satisfied. In this paper some of our previous works results have been shown.

r= Geometric mean of VL (visibility level);
 σ = normalised newly saturated pixels in the restored image ;
e= rate of new visible edge ;

Table I. Parametric Evaluation

Sl. No.	PSNR in dB	CNR	Visible Edge in the original	Visible Edge in restored Image (VERI)	r	σ in %	e	Time CPU (T)
histeq	13.1978	57.5534	25658	93689	3.1839	0.6927	2.6515	0.042s
imadjust	15.7788	58.0879	25658	77871	2.9118	0.35778	2.135	0.033s
adapthisteq	22.0892	61.2216	25658	87877	3.3127	0	2.4249	0.316s
He	8.7759	74.2366	25658	142850	5.4482	0.087619	4.5675	30minute
Tan	9.1426	50.7732	25658	18512	4.7412	0.0028571	0.27851	16.530mints
Tarel	10.2917	61.8767	25658	78045	2.3657	0.0	2.0417	26.76s
Fattal	11.7701	38.0591	25658	55301	4.7711	0.0	1.1553	16.167s
D Berman	15.1094	60.4885	25658	120981	4.9616	9.5238e-05	3.7151	3.471s
Propo Meth I	9.9767	70.7794	25658	156462	5.098	0.35524	5.8146	0.383 sec.
Prop Metd II	10.8262	82.1917	25658	153281	6.7671	0.33937	4.974	0.498s
LaMs	8.4943	66.6353		140969	5.1903	2.3787	4.4942	1.681

In table II different images have been examined with our algorithms . The parameters are above mentioned in table I and Lagrange Multiplier values. It has been perceived that our algorithms performing equally well in different image conditions. Proposed algorithms are rich in colour and pleasing in appearance without ringing/ gibbs effect artifacts. Varied degrees of haze with different outdoor atmospheric conditions are presented for the robustness and visual appearance of the presented algorithms. The images in figure 8 show algorithms' adaptability for different types of atmospheric conditioned images.

Table II: Image set and their performance with the proposed algorithm

Image	LMs	PSNR in dB	CNR	K, before	K, after	Visible Edge in the original	Visible Edge in restored Image (VERI)	r	σ	e	Time CPU (T)
Canon	14.3 950	9.2338	182.6103	0.9 542	0.67 98	4453	23462	7.1648	3.6258e-07	4.2688	0.99527
City_1	39.7 893	11.5401	128.4853	0.9 442	0.85 98	12466	16336	1.7262	1.2750e-06	0.3104	0.579719
City_2	9.07 37	13.5766	177.0917	0.9 422	0.85 74	13671	17597	1.8882	9.9080e-07	0.2872	0.439645
Cones	68.3 063	12.5014	249.0326	0.7 936	0.65 33	9545	11115	3.1036	1.4260e-07	0.1645	1.545280
Lake	11.6 607	16.5402	185.1043	0.5 212	0.50 335	8965	9571	1.4812	1.0827e-07	0.0676	0.277818
Mountain	102. 2181	12.4940	80.4337	0.9 242	0.81 04	5609	15095	4.2541	1.6914e-06	1.6912	0.449133
Ny_1	9.31 24	10.4048	97.1320	0.8 411	0.78 02	26712	29152	1.6655	2.3864e-07	0.0913	0.8170829
Ny_2	15.1 577	12.3916	243.3369	0.8 293	0.68 64 5	43315	44351	2.3405	6.5406e-08	0.0239	1.513777
Pumpkins	465. 7894	12.7700	192.8367	0.7 214	0.55 94	11800	13583	2.0763	9.2231e-08	0.1511	0.537310
Stadium	20.3 356	11.8680	223.7106	0.7 262	0.41 79	17275	25900	3.6818	3.6420e-10	0.4993	0.699850
Toys	16.0 282	9.0041	86.8168	0.8 239	0.58 30	5069	9867	3.6117	7.4749e-08	0.9465	0.472317
Trees	46.0	11.0747	64.5640	0.6	0.60	14937	19535	2.5897	2.4664e-08	0.3078	0.853595

	972			796	64						
Average	-	11.94994 1666667	159.2629 1	-	-	14484.75	19630.33 33	2.9653	4.22e-07	0.734133	0.7650664
Max	-	16.5402	249.0326	-	-	43315	44351	7.1648	1.69e-06	4.2688	1.54528
Min	-	9.0041	64.564	-	-	4453	9571	1.4812	3.6258e-07	0.0239	0.277818
SD	-	2.012862 1970889	65.48862 425963	-	-	10969.23 1638998	9986.005 2376343	1.599899 2939898	5.6995411 118748E-7	1.2097142 249559	0.41034
MAD(Mean Absolute Deviation)	-	1.429025	56.48045 6944444	-	-	7383.333 3333333	7390.611 1111111	1.164916 6666667	4.4842065 833333E-7	0.7840166 6666667	0.3166121 4305556

5.3 Computational Performance

Table III. Time Complexity of the proposed algorithm in terms of Big(O)

Proposed Algorithm	Time Complexity	He et. al. Algorithm	Time Complexity
Get Input Hazy Image		Get Input Hazy Image	
Depth Map with LaM	O(n)	Dark Channel prior	O(n ²)
Average of highest 1% pixel intensity have been considered as Airlight of the image	O(n ²)	Average of highest 1% pixel intensity have been considered as Airlight of the image	O(n ²)
Transmission Estimation from step-II recovery of image	O(n)	Transmission Estimation from step-II	O(n)
-	O(n)	Scene Radiance recovery	O(n)
-	-	Soft Matting	O(n ⁷)
-	-	Scene Radiance recovery	O(n)
Total time	O(n)	Total time	O(n⁷)

It is evident from table III that time complexity of the proposed algorithm is Big (O (n)) whereas that of He et. Al. is of the order of Big (O (n⁷)). They are under P complexity class DTM (Deterministic Turing Machine) in polynomial time [23]. Time complexity is also dependent on filter kernel size. Hence it is validated that proposed algorithm is faster than that of the algorithm [4].

7. Potential Application

This algorithm can be used in surveillance, Military, under water, outdoor image post processing, on board moving vehicle. Intel core i3, 3110M CPU @ 2.40 GHz, 4.0 GB RAM, Intel HD Graphics 4000, 6 years old has been used for the research. Matlab2014a is used as software for experiment.

8 . Conclusion

Particles suspended in the air causes hindrance in the path of light travel. This effect produces serious artifacts and degradation in image formation process at the digital image reconstruction system. As a result visibility becomes almost nil or poor. From that point of view, a low complexity, fast, robust visibility improvement for image is presented. The presented novel method is qualitatively and quantitatively analysed. The outcome of the research shows that the proposed method is applicable in real time, both still as well as for video, with no artifacts. The method is applicable for both colour and grey single image with no ground truth. This approach is very simple. We validate the assumptions of our method through a series of experiments and evaluate the anticipated accuracy through which our procedure assess depth map, transmission map of the scene through RLams . Results show a more effective recovery of the clean scene through refined depth map and transmission estimation compared to existing procedures. The methods are equally adaptable for varied natural image conditions. All statistical parameters, those have been applied, are proved best in the proposed algorithms in comparison with other state-of-art work in this area. Time complexity reduced remarkably in comparison to the other existing techniques. PSNR is not the best but also not the worst. Therefore PSNR can be improved in future. The recovered image is natural in look, as some of the other contemporary work output appears painted or dull. Visual appeal is rich in colour and contrast also reasonable than that of the other popular algorithms. The proposed algorithms are fit for any real time application. Depth map estimation is optimised by low complexity regularized LaMs . LaMs reduce noise in Depth Estimation. This in turn provides good transmission estimation. Image recovery optical model finally generates dehazed output image with YCbCr correction in luma channel to get bright output. This RLams technique produces ringing artifacts free and haze free image which is the main

outcome of this algorithm. Robust estimation theory is the heart of any nonlinear filtering.. Another remarkable approach of this paper is its time complexity analysis .This time complexity analysis also shows improvement along with execution time analysis.

Drawback

This is to emphasise that our method produce more visibility than existing procedures. We are not claiming that it is the absolute outcome. More modification possibilities are there to improve the algorithms depending on transmission map and atmospheric light estimations. As shown in eq (4.1.1) that image optical model is based on two important assumptions: atmospheric light (A) and transmission map (t) estimation. These two estimations are based on priors. Weather condition of each image is unique. Therefore no one method can be claimed to be optimally solve the problem.

Reference

- [1] J Mao, Study of Image Dehazing with the self-adjustment of the Haze Degree, Ph.D. Thesis, Division of Production and Information Systems Engineering, Muroran Institute of Technology, 2015
- [2] H. Koschmieder, Theorie der horizontalensichtweite, Beitr.Phys. Freien Atm., vol. 12, 1924, pp. 171–181.
- [3] S Roy, S S Chaudhuri, Modeling of Ill-Posed Inverse Problem, IJMECS, 2016, 12, pp- 46-55
- [4] K.,He, J., Sun, and X., Tang.,: Single image haze removal using dark channel prior”, IEEE Conference on Computer Vision and Pattern Recognition, Miami, FL, 2009, pp- 1956 – 1963
- [5] R Tan, Visibility in Bad Weather from A Single Image, 2008CPVRIEEE Explore, DOI: 10.1109/CVPR.2008.4587643, ISSN: 1063-6919.
- [6] Tarel, J.-P. , Hautiere, N.: Fast visibility restoration from a single color or gray level image, IEEE 12th International conference on Computer Vision (2009) 2201 – 2208.
- [7] R Fattal, Single Image Dehazing, ACM Transaction on Graphics(TOG), vol-27, Issue-3, August 2008.
- [8] D Berman, T Treibitz, S Avidan, Non-local Image Dehazing, CVPR2016.
- [9] D Das, S Roy, S S Chaudhuri, Dehazing Technique based on Dark Channel Prior model with Sky Masking and its quantitative analysis, CIEC16, IEEE Explore, IEEE Conference ID: 36757 , IEEE Xplore Compliant ISBN No.: 978-1-5090-0035-7, IEEE Xplore Compliant Part No.: CFP1697V-ART, 978-1-5090-0035- 7/16/\$31.00©2016IEEE
- [10] S Roy, S S Chaudhuri, Development of Real Time Visibility Enrichment Algorithms NCECERS2016
- [11] S K Datta, M Hore, S Roy, Objective Evaluation of Dehazed Image by DCP , NCECERS2016-mainak
- [12] S K Datta, M Hore, S Roy, Mathematical Modelling of Image Formation through Atmosphere, NSAMTM2016
- [13] M Hore, S K Datta, S Roy, Subjective & Objective Evaluation of Dehazed Image by DCP , IC2C2SE2016
- [14] D Roy, S Banerjee, S Roy, , S S Chaudhuri, Removal of the Artifacts Present in the Existing Dehazing Techniques, IC2C2SE2016
- [15] S Roy, S S Chaudhuri, Modelling and control of sky pixels in visibility improvement through CSA , IC2C2SE2016
- [16] S Roy, S S Chaudhuri, Modeling of Haze Image as Ill posed Inverse Problem & its solution, IJMECS, vol:8, no:12, pp:46-55, December 2016.
- [17] I Pitas, A N Venetsanopoulos, Order Statistics in Digital Signal Processing, Proceedings of IEEE, Vol-80, No-12, December 1992, pp- 1893-1921.
- [18] R C Gonzalez, R E Woods, Digital Image Processing, ,3rd Edition, Pearson.
- [19] N Hautiere, J P Tarel, D Aubert, E Doumont, Blind contrast enhancement assessment by gradient rationing at visible edges , Image Analysis and stereology.
- [20] V Radhika, G Padmavati, Performance of various order statistics filters in impulse and mixed noise removal for RS images, Signal & Image Processing : An International Journal(SIPIJ) Vol.1, No.2, December 2010
- [21] C Mythili, V Kavitha, Efficient technique for color image noise reduction, The Research Bulletin of Jordan ACM , Vol II(III)
- [22] X Xiang, D H Brainard, Estimation of Saturated Pixel Values in Digital Colour Imaging, Optical Society of America, Vol-21, No-8, pp- 2301-2310.
- [23] M Sipser, Introduction to the theory of computation, Cengage Learning, 3rd Edition, 2013.
- [24] I Stoganovic, P Stanimirovic, M Miladinovic, Applying the algorithm of Lagrange Multipliers in digital image restoration.
- [25] T Chan, S Esedoglu, F Park, A Yip, Recent Trends in Total Variation Image Restoration, Mathematical Model in Computer Vision: A Hand Book, Department of Mathematics, University of Californis, 1-18, 2004.
- [26] A Buades, B Coll, J M Morel, A Reviw of Image Denoising Algorithms, with a new one, ” Multiscale Model. Simul., vol. 4, no. 2, pp. 490–530, 2005.
- [27] G Landi, Lagrangian Methods for the regularization of the discrete ill-posed problems, Computational Optimization and Applications, 39(3), 347-368, Springer US, 2008.
- [28] D Baraff, Linear Time Dynamics using Lagrange Multipliers, Carnegie Mellon University, 1996.
- [29] M Subbarao, On the Depth Information in The Point Spread Function of a Defocused Optical System, State University of New York, 1999.
- [30] E Pontelli, K Vellaverde, Complexity of Algorithms, Department of Computer Science, New Maxico State University.
- [31] Sangita Roy, Sheli Sinha Chaudhuri, Low Complexity Single Colour Image Dehazing Technique, Intelligent Multidimensional Data and Image Processing, 2018, IGI Global (formerly Idea Group Inc.).
- [38] H. Koschmieder, Theorie der horizontalensichtweite, Beitr.Phys. Freien Atm., vol. 12, 1924, pp. 171–181.
- [39] E J McCartney , Optics of the Atmosphere: Scattering by Molecules and Particles, New York, NY, USA: Wiley, 1976.

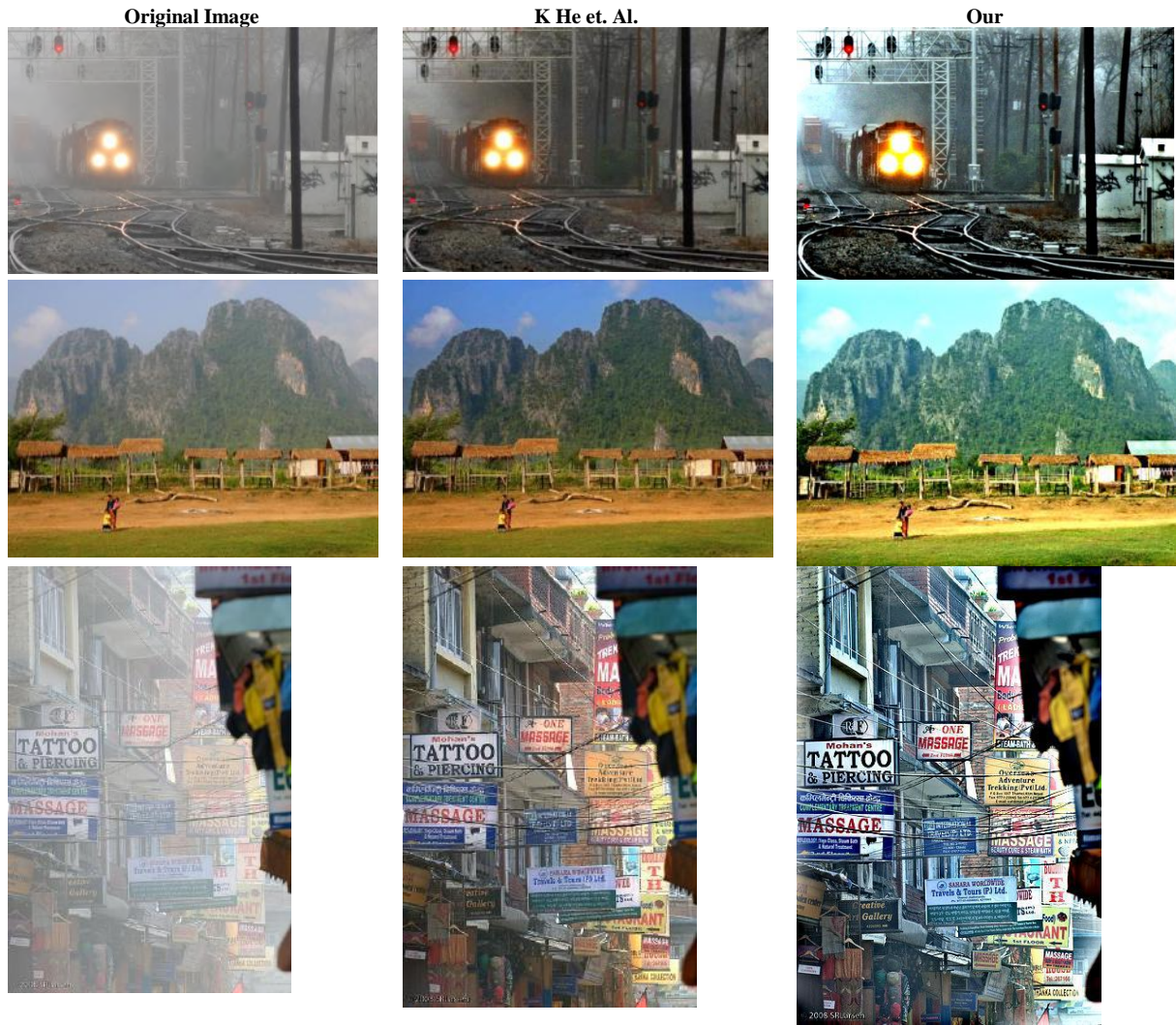


Fig. 9 Left column: Original Image, Middle column: Clean image with algorithm He et. Al., Right column clean image with our algorithm.

